Supporting Information for

Exploring the Design of Superradiant J-Aggregates from Amphiphilic Monomer Units

Austin D. Bailey[a], Arundhati P. Deshmukh[a], Nadine C. Bradbury[a], Monica Pengshung[a], Jillian A. Williams[a], Timothy L. Atallah[c], Ulugbek Barotov[b], Daniel Neuhauser[a], Ellen M. Sletten[a]*, and Justin R. Caram[a]*

[a]*Department of Chemistry and Biochemistry, University of California, Los Angeles, Los Angeles, California-90095, United States.*

[b]*Department of Chemistry, Massachusetts Institute of Technology, Cambridge, MA 02139*

[c]*Department of Chemistry and Biochemistry, Denison University, Granville, OH, 43023, USA*

Email: jcaram@chem.ucla.edu

Table of Contents

1. General experimental information

Chemical reagents were purchased from Fisher Scientific or Sigma-Aldrich and were used without purification unless specified. 5,6-Dichloro-2-methylbenzimidazole, 2-methylbenzimidazole and glutaconaldehydedianil hydrochloride were purchased from TCI America. Anhydrous DMSO was obtained from a Sure-Seal™ bottle from Sigma-Aldrich. Anhydrous DMF was obtained from a Grubb's-type Phoenix Solvent Drying System. Dry ethanol was prepared by drying over molecular sieves for 48 h. Thin layer chromatography was performed using Silica 60 F_{254} plates (Sigma-Aldrich). Flash chromatography was performed using Silica Gel 60 from Fisher Scientific (40-63 μm). Solvents were removed using a Buchi Rotavapor RE111 attached to a Cenco Pressovac pump. Bath sonication was performed using Branson 2510 model sonicator. Masses were measured on a Mettler Toledo AB204-S balance. Unless otherwise specified, all reactions were performed under Ar atmosphere on a ChemGlass CG-4441-02 Schlenk line.

Nuclear magnetic resonance (^{1}H, ^{13}C) spectra were taken on a Bruker Avance 400 spectrometer and processed using TopSpin 4.0.4.

Absorbance spectra were measured on a Cary 60 UV-vis spectrophotometer with a 4800 nm/min. rate after blanking with the appropriate solvent.

DMSO = dimethylsulfoxide
MeOH = methanol
EtOH = ethanol
H_2O = water
MQ H_2O = MilliQ H_2O
DMF = dimethylformamide

2. Synthetic Procedures

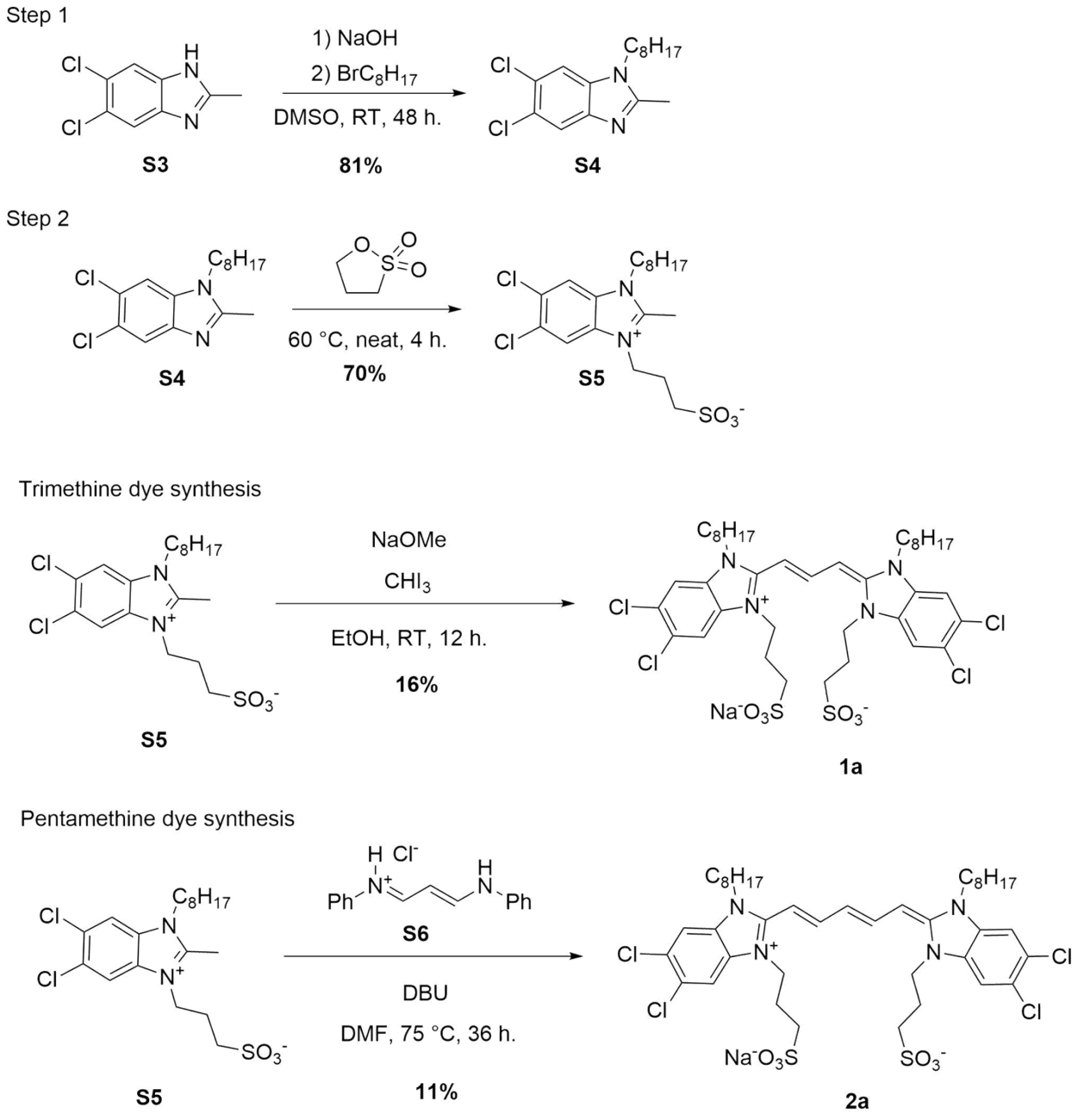

Scheme 1. Synthesis of tetrachlorobenzimidazole heterocycles and dyes.

Synthesis of **S4** (5,6-dichloro-2-methyl-1-octyl-1H-benzo[d]imidazole)

5,6-dichloro-2-methylbenzimidazole (**S3**, 1.00 g, 5.0 mmol, 1 eq.) and ground NaOH (269 mg, 6.71 mmol, 1.35 eq) was evacuated and subsequently purged with argon for three cycles before adding anhydrous DMSO (9 mL). After stirring for 4 h. bromooctane (1.72 mL, 9.95 mmol, 2.0 equiv.). was added dropwise and allowed to stir for 48 h. The reaction was quenched with H_2O (20 mL) at which point a pink precipitate formed. The reaction mixture was suction filtered and washed with water and acetone to yield the product

as a white, powdery solid (1.26 g, 4.02 mmol, 81%). ^{1}H NMR (400 MHz, CD_3OD): δ 7.61 (s, 2H), 4.13 (t, *J* = 14.7 Hz, 2H), 1.74 (t, *J* = 6.5 Hz, 2H), 1.25 (m, 10H), 0.852 (t, *J* = 6.95 Hz 3H). ^{1}H-NMR matches literature.[1]

Synthesis of **S5** (2-(5,6-dichloro-2-methyl-1-octyl-1H-benzo[d]imidazol-3-ium-3-yl)ethane-1-sulfonate)

5,6-dichloro-2-methyl-1-octyl-1H-benzo[d]imidazole (**S4**, 135 mg, 430 μmol, 1 eq.) and propane sultone (158 mg, 1.29 mmol, 3 eq.) were evacuated and subsequently purged with argon for three cycles before heating to 60 °C. After stirring for 4 h, the reaction was allowed to cool and acetone (25 mL) was added. The precipitate was suction filtered and washed using acetone to yield the product as a white, flaky solid (131 mg, 301 mmol, 70%) ^{1}H NMR (400 MHz, CD_3OD): δ 8.36 (s, 1H), 8.24 (s, 1H), 4.67 (t, *J* = 14.3 Hz, 2H), 4.45 (t, *J* = 7.5 Hz, 2H), 2.96 (s, 5H), 2.30 (q, 2H), 1.30 (m, 10 H), 0.89 (m, 3H). ^{1}H-NMR matches literature.[1]

Synthesis of **1a** (sodium 3-(5,6-dichloro-2-((1E,3E)-3-(5,6-dichloro-1-octyl-3-(3-sulfonatopropyl)-1,3-dihydro-2H-benzo[d]imidazol-2-ylidene)prop-1-en-1-yl)-1-octyl-1H-benzo[d]imidazol-3-ium-3-yl)propane-1-sulfonate).

3-(5,6-dichloro-2-methyl-1-octyl-1*H*-benzo[*d*]imidazol-3-ium-3-yl)propane-1-sulfonate (**S5**, 300 mg, 689 μmol, 1 eq), sodium methoxide (93 mg, 1.72 mmol, 2.5 eq.) and iodoform (163 mg, 413 μmol, 0.6 eq.) were added to a 25 mL Schlenk flask which was evacuated and subsequently purged with argon for three cycles. Anhydrous ethanol (8 mL) was added and the mixture was immediately frozen with liquid nitrogen and underwent three freeze, pump, thaw cycles. The mixture was allowed to warm to R.T. before heating to 60 °C in an oil bath and stirring for 10 min. The mixture was returned to R.T. and allowed to stir for 15 h. The crude reaction mixture was then suction filtered and washed with cold acetone (10 mL) and cold H_2O (10 mL). The crude product was recrystallized in a 1:1 ratio of DMF:H_2O to give the product as a glittery red solid with an orange tinge (100 mg, 111 μmol, 16%). ^{1}H NMR (400 MHz, MeOD): δ 7.96 (t, 1H), 7.82 (s, 2H), 7.69 (s, 2H), 5.88 (d, 1H), 4.43 (t, 3H), 4.29 (t, 3H), 2.93 (t, 3H), 2.24 (m, 3H), 1.84 (m, 3H), 1.34-1.22 (m, 18H), 0.84 (s, 6H). ^{1}H-NMR matches literature.[1]

Synthesis of **2a** (sodium 3-(5,6-dichloro-2-((1E,3E,5E)-5-(5,6-dichloro-1-octyl-3-(3-sulfonatopropyl)-1,3-dihydro-2H-benzo[d]imidazol-2-ylidene)penta-1,3-dien-1-yl)-1-octyl-1H-benzo[d]imidazol-3-ium-3-yl)propane-1-sulfonate).

3-(5,6-dichloro-2-methyl-1-octyl-1*H*-benzo[*d*]imidazol-3-ium-3-yl)propane-1-sulfonate (**S5**, 120 mg, 0.28 mmol, 1 eq.), malonaldehyde bis(phenylimine) HCl (**S6** 34 mg, 0.13 mmol, 0.46 eq.) were added to a 25 mL Schlenk flask which was evacuated and subsequently purged with argon for three cycles then dissolved in dimethylformamide (anhydrous, 8 mL). To this solution, 1,8-diazabicycloundec-7-ene (DBU, 0.3 mL, 2 mmol, 7 equiv.) was added and the mixture was heated to 75 °C for 36 h. The mixture was cooled to rt and concentrated to give a green residue which was dissolved in DI water (150 mL) and washed with toluene (100 mL). The aqueous layer was basified with saturated $NaHCO_3$ and a fine blue/green precipitate was formed. The precipitate was collected by suction filtration and purified via silica gel chromatography twice using a dichloromethane/methanol solvent system with a gradient elution from 0 to 10% methanol. This procedure resulted in a pure blue powder (30 mg, 0.03 mmol, 11%). ^{1}H NMR (600 MHz, MeOD): δ 7.94 (t, *J* = 13.4 Hz, 2H), 7.78 (s, 2H), 7.64 (s, 2H), 6.29 (t, *J* = 11.2 Hz, 1H), 5.68 (d, *J* = 13.4 Hz, 2H), 4.48 (bs, 4H), 4.29 (bs, 4H), 3.02 (bs, 4H), 2.29 (bs, 4H), 1.84 (bs, 4H), 1.44–1.21 (m, 20H), 0.90 – 0.84 (m, 6H). ^{13}C NMR (151 MHz, MeOD): δ 150.4, 149.8, 134.0, 133.8, 128.59, 128.58, 120.6, 112.32, 112.28, 88.4, 49.2, 46.1, 45.3, 33.1, 30.5, 30.4, 29.1, 27.7, 25.1, 23.9, 14.6.HRMS (ESI$^-$): Calculated for $C_{41}H_{55}Cl_4N_4O_6S_2$ $[M^-]^-$: 905.2311; found: 905.2307.

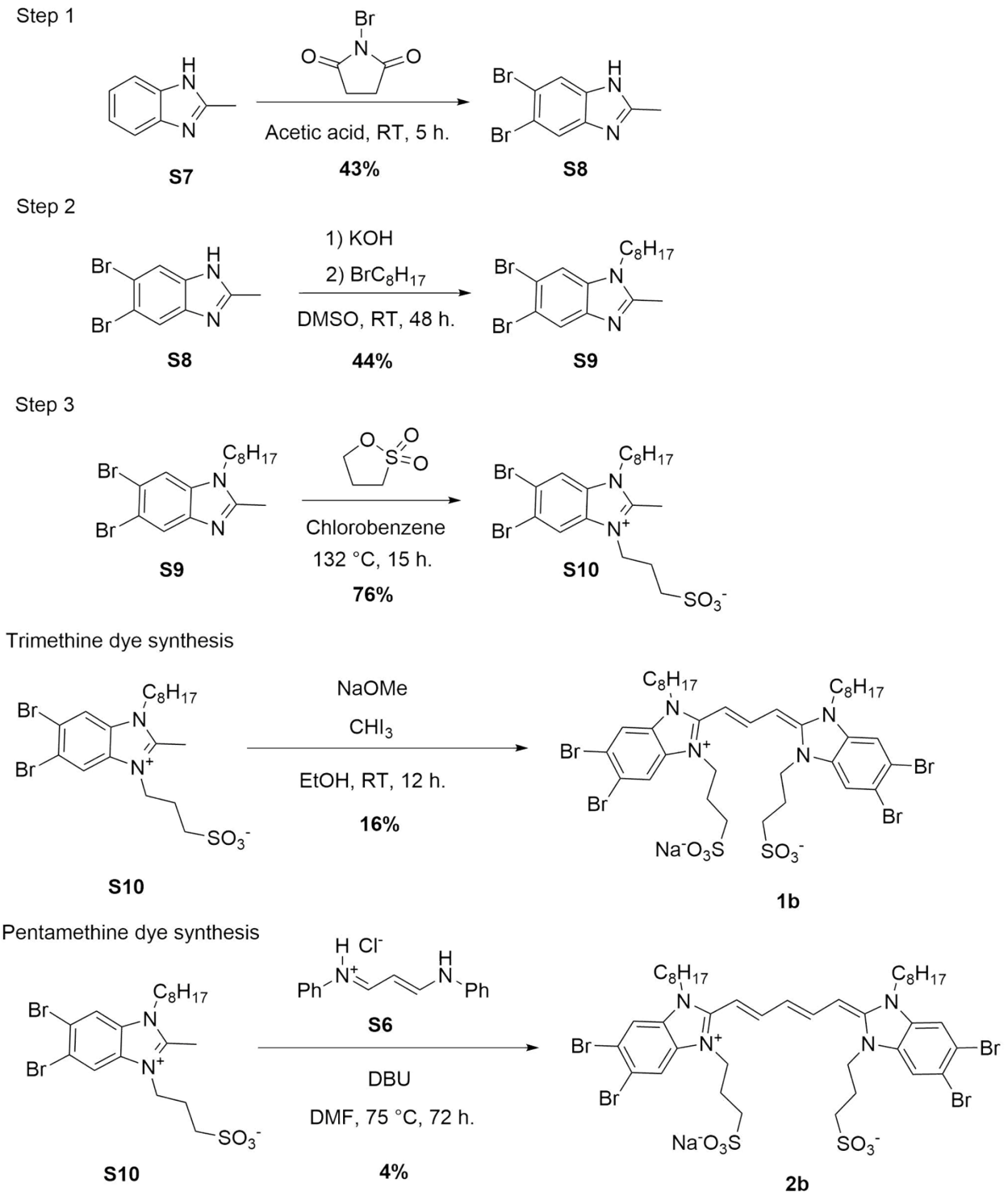

Scheme 2. Synthesis of tetrabromobenzimidazole heterocycles and dyes.

Synthesis of **S8** (5,6-dibromo-2-methyl-benzimidazole).

2-methyl-benzimidazole (**S7**, 1.500 g, 11.35 mmol, 1 eq.) and *N*-bromosuccinimide (4.240 g, 23.83 mmol, 2.1 eq.) were dissolved in glacial acetic acid (16 mL), heated to 60 °C, and stirred for 5 h. The reaction mixture was suction filtered and washed several times with saturated aqueous $NaHCO_3$ and water to yield

2 as a white solid (1.43 g, 4.93 mmol, 43.3%). ^{1}H NMR (400 MHz, CD_3OD): δ7.78 (s, 2H), 2.54 (s, 3H). ^{1}H-NMR matches literature.[1]

Synthesis of **S9** (5,6-dibromo-2-methyl-1-octyl-1H-benzo[d]imidazole).

5,6-dibromo-2-methylbenzimidazole (**S8**, 5.32 g, 18.34 mmol, 1 eq.), KOH (2.06 g, 36.7 mmol, 2 eq.) were evacuated and subsequently purged with argon for three cycles. The flask was purged 3x using argon and vacuum before adding dry DMF (8 mL), cooling to 0 °C, and allowing the mixture to stir for 4 h. After stirring, $C_8H_{17}Br$ (6.3 mL, 36.7 mmol, 2 eq.) was added and the reaction was left to stir for 48 h. The mixture was then suction filtered and washed using cold acetone yield **3** as a white, powdery solid (3.23 g, 8.03 mmol, 44%) ^{1}H NMR (400 MHz, CD_3OD): δ 7.85 (d, *J* = 9.81, 2H), 4.17 (t, *J* = 14.69, 2H), 2.57 (s, 2H), 1.76 (m, 3H), 1.32-1.24 (m, 10H), 0.86 (t, *J* = 6.94, 3H). ^{1}H-NMR matches literature.[1]

Synthesis of **10** (3-(5,6-dibromo-2-methyl-1-octyl-1H-benzo[d]imidazol-3-ium-3-yl)propane-1-sulfonate.)

5,6-dibromo-2-methyl-1-octyl-1H-benzo[d]imidazole (**S9**, 312 mg, 775 µmol, 1 eq.), 1,3-propanesultone (95 mg, 775 µmol, 1 eq.) dissolved in chlorobenzene (15 mL). The mixture was heated to 132 °C and allowed to reflux for 15 h. After refluxing the reaction was cooled to R.T. and a white precipitate formed. The solid was suction filtered and washed 3x with diethyl ether (10 mL) to yield a white, powdery solid (309 mg, 0.59 mmol, 76%) ^{1}H NMR (400 MHz, CD_3OD): δ 8.49 (s, 1H), 8.37 (s, 1H), 4.64 (t, *J* = 15.6 Hz, 2H), 4.41 (t, *J* = 15.3, 2H), 2.91 (t, *J* = 13.3, 2H), 2.27 (q, *J* = 14.2 Hz, 2H), 1.847 (q, *J* = 14.9, 2H), 1.37 (m, 10H), 0.87 (t, 13.7, 3H). ^{1}H-NMR matches literature.[1]

Synthesis of **1b** (sodium 3-(5,6-dibromo-2-((1E,3E)-3-(5,6-dibromo-1-octyl-3-(3-sulfonatopropyl)-1,3-dihydro-2H-benzo[d]imidazol-2-ylidene)prop-1-en-1-yl)-1-octyl-1H-benzo[d]imidazol-3-ium-3-yl)propane-1-sulfonate).

3-(5,6-dibromo-2-methyl-1-octyl-1*H*-benzo[*d*]imidazol-3-ium-3-yl)propane-1-sulfonate (**S10**, 313 mg, 597 µmol, 1 eq.), sodium methoxide (80 mg, 1.49 mmol, 2.5 eq.) and iodoform (141 mg, 358 µmol, 0.6 eq.) were added to a 25 mL Schlenk flask which was evacuated and subsequently purged with argon for three cycles. Dry ethanol (8 mL) was then added and the mixture was immediately frozen with liquid nitrogen and underwent three freeze, pump, thaw cycles to ensure an O_2 free environment. The mixture was allowed to warm to R.T. before heating to 60 °C in an oil bath and stirring for 10 min. After heating, the mixture was returned to R.T. and allowed to stir for 15 h. The reaction mixture was then suction filtered and washed with 10 mL cold acetone and 10 mL cold H_2O. The crude product was recrystallized in a 1:1 ratio of DMF:H_2O to give the product as a glittery red solid with an orange tinge (168 mg, 155 µmol, 26%). ^{1}H NMR (400 MHz, DMSO-d6): δ 8.12 (s, 2H), 8.04 (s, 2H), 7.86 (t, *J* = 13.9 Hz, 1H) 5.87 (d, *J* = 13.5 Hz, 2H), 4.36 (t, *J* = 6.80, 4H), 4.2611 (t, *J* = 6.78, 4H), 1.99 (m, 4H), 1.69 (m, 4H), 1.21 (m, 20H), 0.76 (t, *J* = 13.7, 6H). ^{1}H-NMR matches literature.[1]

Synthesis of **2b** (sodium 3-(5,6-dibromo-2-((1E,3E,5E)-5-(5,6-dibromo-1-octyl-3-(3-sulfonatopropyl)-1,3-dihydro-2H-benzo[d]imidazol-2-ylidene)penta-1,3-dien-1-yl)-1-octyl-1H-benzo[d]imidazol-3-ium-3-yl)propane-1-sulfonate).

3-(5,6-dibromo-2-methyl-1-octyl-1*H*-benzo[*d*]imidazol-3-ium-3-yl)propane-1-sulfonate (**S10**, 120 mg, 0.28 mmol, 1 eq.) and malonaldehyde bis(phenylimine) HCl (**S6**, 34 mg, 0.13 mmol, 0.46 eq.) were added to a 25 mL Schlenk flask which was evacuated and subsequently purged with argon for three cycles. These

reagents were dissolved in dimethylformamide (DMF, anhydrous, 8 mL). To this solution, 1,8-diazabicycloundec-7-ene (DBU, 0.3 mL, 2 mmol, 7 equiv.) was added and the mixture was degassed via 3 cycles of freeze, pump, thaw. The reaction was then heated to 75 ^{o}C for 72 h at which point the mixture was cooled to R.T. and evaporated to dryness. The green residue was dissolved in DI water (150 mL) and washed with toluene (1 x 100 mL). The aqueous layer was basified with saturated $NaHCO_3$ and a fine blue/green precipitate was formed. The precipitate was collected by suction filtration and twice chromatographed on silica gel using a dichloromethane/methanol solvent system with a gradient elution from 0 to 10% methanol. This procedure yielded the product as a blue powder. (30 mg, 0.03 mmol, 11%). ^{1}H NMR (400 MHz, MeOD): δ 7.95 (t, *J* = 12.9 Hz, 1H), 7.91 (s, 2H), 7.77 (s, 2H), 6.29 (t, *J* = 11.7 Hz, 1H), 5.70 (d, *J* = 14.2 Hz, 1H), 4.47 (t, *J* = 15.9 Hz, 3H), 4.28 (t, *J* = 6.94 Hz, 2H), 3.02 (t, *J* = 6.48 Hz, 3H), 2.28 (m, 4H), 1.83 (t, *J* = 7.92 Hz, 4H), 1.47-1.18 (m, 20 H), 0.9-0.82 (m, 6H). ^{13}C NMR (500 MHz, DMSO-d6) 133.1, 118.2, 113.7, 54.4, 44.5, 43.6, 31.5, 31.5, 29.0, 28.9, 27.5, 26.1, 23.5, 22.3, 22.2, 13.1 HRMS (ESI): calcd for $C_{41}H_{57}Br_4N_4O_6S_2^+$: 1081.0453 found: 1081.0470.

3. Heptamethine C8S3 Synthesis and Degradation

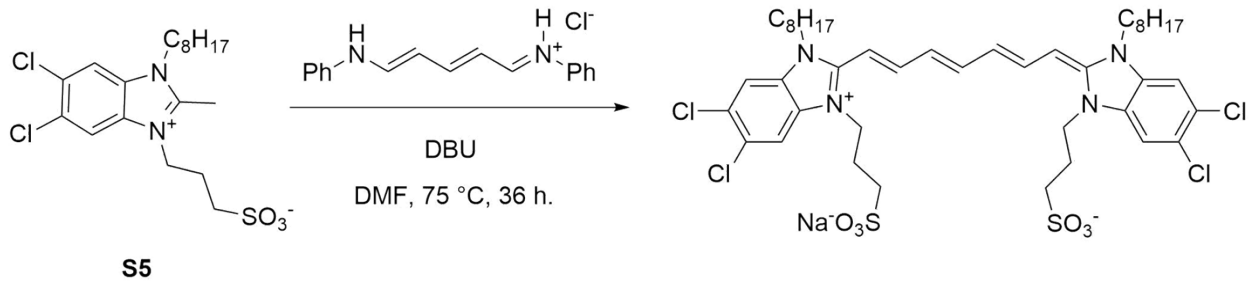

Scheme 10. Synthesis of C8S3 Cy7-Cl.

3-(5,6-dichloro-2-methyl-1-octyl-1*H*-benzo[*d*]imidazol-3-ium-3-yl)propane-1-sulfonate (**S5**, 300 mg, 0.69 mmol, 10 eq.) and glutaconaldehydedianil Hydrochloride (20.5 mg, 0.082 mmol, 1 eq.) were dissolved in dimethylformamide (anhydrous, 8 mL). To this solution, 1,8-diazabicycloundec-7-ene (DBU, 0.143 mL, 0.96 mmol, 14 eq.) was added and the mixture was degassed via 3 cycles of freeze, pump, thaw. The reaction was then heated to 75 °C for 72 h., at which point the mixture was cooled to R.T. and evaporated to dryness. The residue was dissolved in 20 mL dichloromethane, to which 100 mL of sat. aqueous $NaHCO_3$ was added. The aqueous layer was washed with DCM until colorless and at which point layers were combined and evaporated. The resulting solid was twice chromatographed on silica gel using a dichloromethane/methanol solvent system with a gradient elution from 0 to 10% methanol. The procedure provided a compound with appropriate absorbance ~730 nm which degraded quickly in methanol (shown in SI Figure 1). Due to the instability of this compound, aggregation attempts were unsuccessful and therefore the C8S3-Cy7 analogs were not pursued.

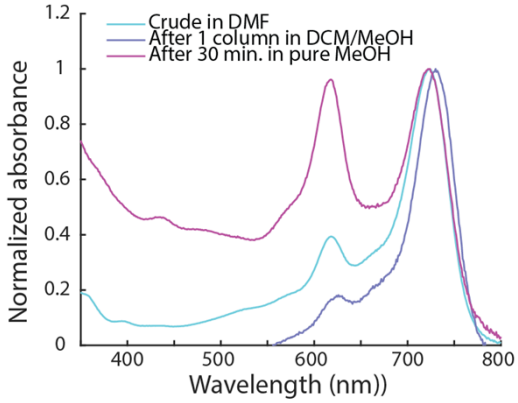

Figure S1. Absorption of C8S3 Cy7-Cl at various stages of degradation.

We also note that the absorption features at 600 and 730 nm were found to change in relative intensity in different solvents (e.g. acetone, DCM). This led us to believe that the dye may be photodegrading to a blueshifted form, similar to what was published by Schnermann and coworkers.[2]

4. Aggregation procedures for dye monomers

We prepared aggregates of each chromophore first by weighing the dye monomers on a Sartorius MSE6.6S-000-DM Cubis Micro Balance and creating a stock solution of the dye in methanol; the stock concentration typically ranged from 0.1 to 1 mM depending on the desired final concentration of dye. To a small volume of this stock solution was added ultrapure H_2O (resistivity 18.6 MΩ at room temperature). The final concentration in each solution was varied and UV-Vis absorption was used to characterize the kinetics and end-result of aggregation. Most samples would have a final concentration of approximately 0.1 mM dye and were 10-30% methanol by volume. These solutions were then parafilmed, wrapped in foil, and stored in a dry place for 24 h to allow time for assembly. The resulting aggregates were characterized immediately to prevent possible degradation of these materials. MATLAB code for calculating dye weights and MeOH/H_2O volumes for variable concentration and %MeOH samples is available upon request. The exact recipes for each aggregate used in this work are given in Table S1.

Table S1. Aggregate formation conditions.

Compound	Morphology	Dye concentration (mM)	%MeOH	%H_2O	Time
1a	DWNT	0.2	20	80	24 h.
1a	Bundles	0.2	20	80	10 weeks
1b	DWNT	0.2	20	80	24 h.
1b	Bundles	0.2	20	80	10 weeks
2a	KI	0.1	10	90	24 h.
2a	Bundles	1	10	90	24 h.
2b	KI	0.1	10	90	24 h.
2b	Bundles	1	10	90	24 h.

5. Cryo-EM conditions and sample preparation

CryoEM images were recorded on a FEI TF20 electron microscope equipped with a field-emission gun at 200 kV. CryoEM grids were loaded on to a Gatan 626 cryo-transfer sample holder, and inserted into the microscope, where all images were taken under liquid nitrogen. The images were recorded on a CCD camera with 4k × 4k resolution. Image defocus was used to enhance contrast. Cryo-electron microscopy (CryoEM) samples were prepared on mesh 200 lacey formvar/carbon copper grids obtained from Ted Pella Inc. The grids were plasma-cleaned under a H_2/O_2 gas flow using a Solarus Gatan Plasma cleaner for hydrophilization. Plunge-freezing was done for all samples on a Vitrobot Mark IV by dropping 3.5 or 5.0 µL of the aggregate solution onto the grid, then blotting for 3.0 s with standard blotting paper from Ted Pella. The grid was immediately dropped into liquid ethane maintained close to its freezing point using liquid nitrogen. The frozen grids were stored in liquid nitrogen.[3]

6. Emission Spectra

Photoluminescence spectra were obtained on a Horiba Instruments PTI QM-400 using 1 cm quartz cuvettes. The monomers of **1a** and **1b** were excited at 450 nm, while the monomers of **2a** and **2b** were excited at 532 nm. Aggregates of **1a** and **1b** were excited at 532 nm, while aggregates of **2a** and **2b** were excited at 670 nm.

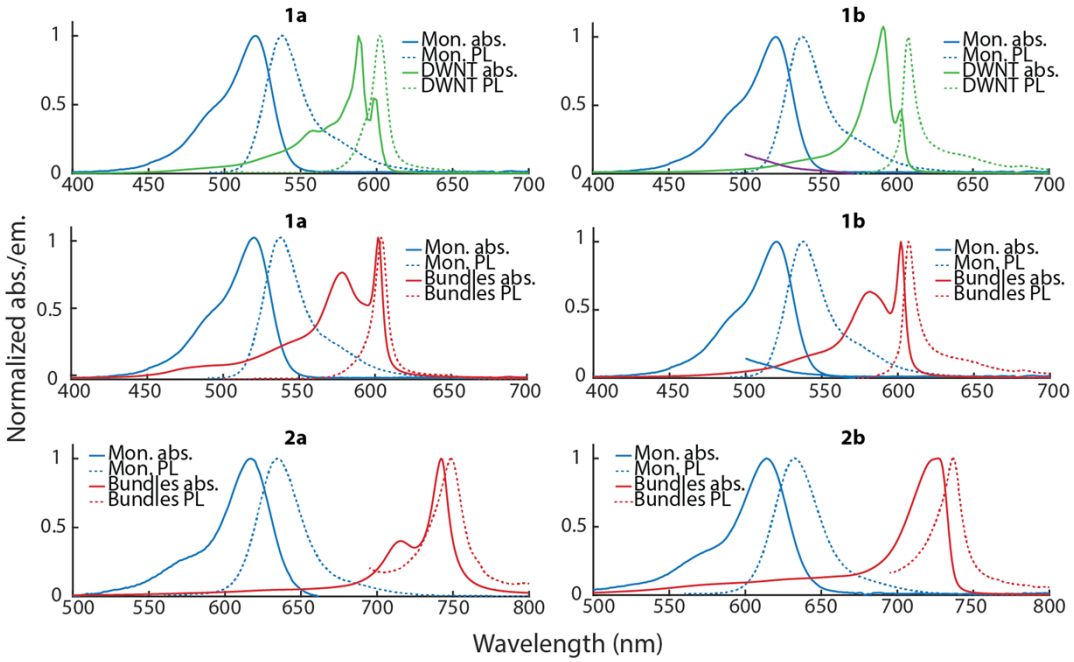

Figure S4. Emission spectra for **1a**, **1b**, **2a**, and **2b** and corresponding aggregates.

7. Quantum Yield measurements

Relative fluorescence quantum yield measurements:

The quantum yields of the trimethine (**1a**/**1b**) and pentamethine monomers (**2a**/**2b**) were evaluated using the relative method against known standards Nile Red (Φ_F = 0.28, methanol), Nile Blue A Perchlorate (Φ_F = 0.27, ethanol), respectively. For the relative QY measurements, absorbance spectra were collected on a JASCO V-770 UV-Visible/NIR spectrophotometer and JASCO V-730 UV-Visible/NIR with a 2000 nm/min scan rate after blanking with the appropriate solvent. Photoluminescence spectra were obtained on a Horiba Instruments PTI QM-400. Quartz cuvettes (1 cm) were used for absorbance and photoluminescence measurements.

The fluorescence quantum yield (Φ_F) of a molecule or material is defined as follows:

$$\Phi_F = \frac{P_E}{P_A} \qquad (1)$$

Where P_E and P_A represent the number of photons emitted and absorbed, respectively. To determine the quantum yield, we used a relative method with either nile red (trimethine monomers) or nile blue A perchlorate (pentamethine monomers) as a known standard in the same region of the electromagnetic spectrum. To compare an unknown to a reference with a known quantum yield, the following relationship was used:

$$\Phi_{F,x} = \Phi_{F,r}\,(m_x/m_r)(\eta_x^2/\eta_r^2)$$

Where m represents the slope of the line (y = mx + b) obtained from graphing integrated fluorescence intensity versus optical density across a series of samples, η is the refractive index of the solvent and the subscripts *x* and *r* represent values of the unknown and reference, respectively.

To obtain a plot of integrated fluorescence intensity versus absorbance for the reference and unknown, five solutions and a solvent blank were prepared with absorbance maxima between 0.01 and 0.1 au. Absorbance and emission spectra (with an excitation wavelength of 450 nm (trimethines) or 532 nm (pentamethines)) were acquired for all samples. Reference and unknown dyes were diluted in methanol to concentrations with optical densities less than 0.1 to minimize effects of reabsorption. The fluorescence traces were integrated, and the raw integrals were corrected by subtracting the integral over an identical range from fluorescence traces of the blank solvent. The integrated fluorescence intensities were then plotted against the baseline corrected absorbance values at the relevant wavelength and the slope and error in slope were obtained (R^2 > 0.99 for all traces).

Absolute fluorescence quantum yield measurements:

Quantum yields of J-aggregates are notoriously difficult to measure due to large reabsorption effects that result from near entirely overlapping absorption and emission. Additionally, the aggregates are not amenable to dilutions due to either disassembling the nanostructures or disordering them to the point where their original photophysics may not be retained.

To minimize these problems, we employed the De Mello method for absolute quantum yield, which has been described in detail elsewhere.[4,5] In short, a short path length cuvette (0.1 or 0.01 mm depending on aggregate concentration) is inserted into a LabSphere 6" QE integrating sphere which uniformly illuminates the sample on all sides from the input excitation beam. We used a variable wavelength superK laser as excitation for the trimethine (565 nm) and pentamethine (700 nm) aggregates and recorded the emission spectrum at three different concentrations for each aggregate.

8. Lifetime measurements and fitting

Time-resolved photoluminescence (TRPL) were recorded at room temperature using a homebuilt, all-reflective epifluorescence setup.[6] The dye solutions were excited via a pulsed output from a 532 nm laser (LDH-P-FA-530B, PicoQuant). The emission was filtered (550 nm longpass dichroic, DMLP550R, Thorlabs; 550 nm longpass filter, FELH0550, Thorlabs, 532 nm notch, NF533-17, Thorlabs) and collected using time correlated single photon counting (TCPSC) histogramming with a Si-avalanche photodiode (PD-050-CTD, Micro Photon Devices) connected to a synchronized photon counter (Picoquant, Hydraharp 400).

We determined the monomer lifetimes by fitting the decay of the TCSPC trace to single exponentials for the **2a** and **2b** dyes and two exponentials for the **1a** and **1b** dyes. For aggregate lifetimes, we fit the TRPL traces to a numerical convolution of a biexponential function with the instrument response function (IRF) and extracted the corresponding rates. The IRF was measured as laser back-scatter from a cuvette with only solvent. MATLAB code for the fitting is available upon request. All monomer fits are available in SI Figure 5. Aggregate fits are available in SI Figure 6.

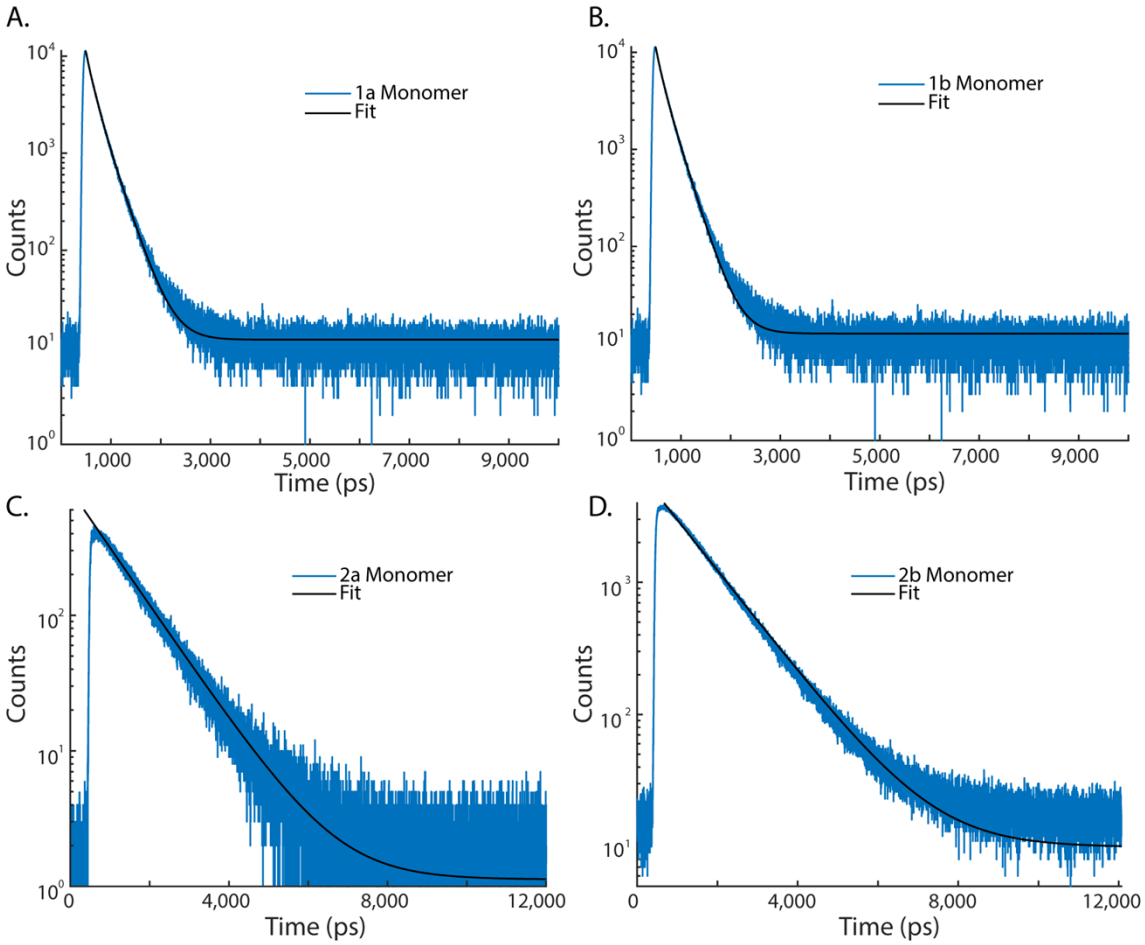

Figure S5. Monomer lifetimes and fittings. A. 1a (100% MeOH) **B. 1b** (100% MeOH) **C. 2a** (100% MeOH) **D. 2b**. (100% MeOH)

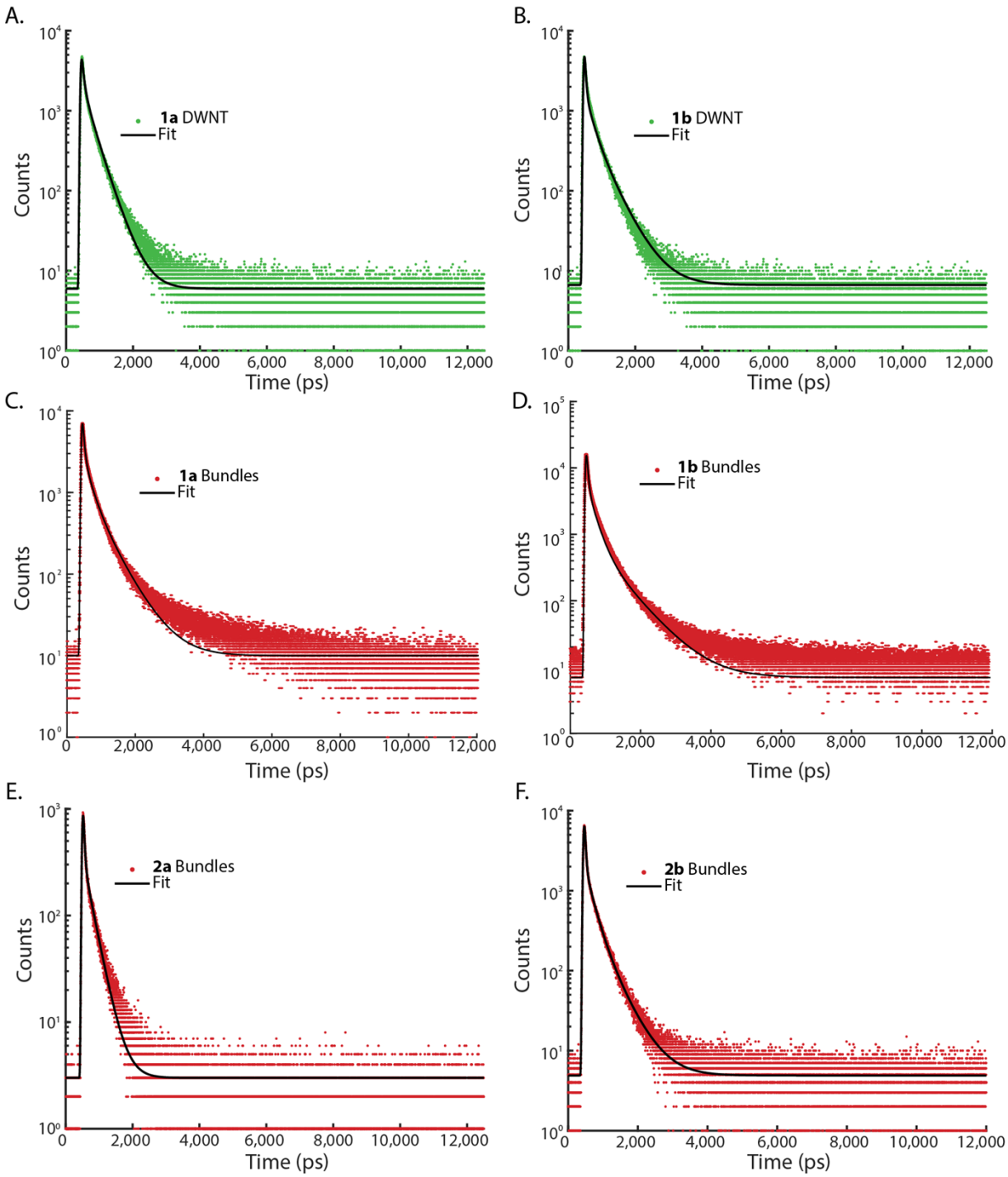

Figure S6. Aggregate lifetimes and fittings. A. 1a DWNT (20% MeOH) **B. 1b** DWNT (20% MeOH) **C. 1a** bundle (20% MeOH) **D. 1b** bundle (20% MeOH) **E. 2a** bundle (10% MeOH) **F. 2b** bundle (10% MeOH).

9. Transition dipole moment analysis

Following the identification of the quantum yields and lifetimes for all monomer and aggregate morphologies, we performed several intermediate calculations to obtain the transition dipole moment (TDM, μ).

For each aggregate we recovered a short and long time components (τ_i) with an associated amplitude factor (A_i). To bring these values forward, we obtained the amplitude-weighted average lifetimes as done by Engelborghs and coworkers.[7] The amplitude-weighted total rate (k_{tot}) was obtained via the same process using the reciprocal of the lifetimes, demonstrated by equation 1.

$$\langle k \rangle_a = \frac{\sum A_i k_i}{\sum A_i} \qquad \text{(Eq 2)}$$

We then obtain the radiative rate (k_r) by multiplying the averaged total rate and quantum yield (Φ_F) as in equation 2.

$$k_r = k_{tot} \Phi_F \qquad \text{(Eq 3)}$$

We must also factor in the energy gap (E_g), taken as the average energy of absorption and emission for a particular monomer or aggregate. E_g is calculated via equation 3.[8]

$$E_g = \nu_{max} + \frac{\nu_{Stokes\ shift}}{2} \qquad \text{(Eq 4)}$$

E_g can be converted into wavelength by performing E_g (nm) = $10^7/E_g$ (cm^{-1}). From k_r and E_g, we calculate TDM using equation 4, where ε_o is the dielectric of free space, $\hbar$ is the reduced Planck's constant, c is the speed of light, n is the index of refraction for the solvent in which quantum yield was measured. Note that E_g is used in Joules for equation 5.

$$\mu_{21} = \sqrt{\frac{k_r 3\pi\varepsilon_o \hbar^4 c^3}{n E_g^{\ 3}}} \qquad \text{(Eq 5)}$$

As mentioned in the main text, the superradiance parameter of a given compound is then the ratio of squared transition dipoles for aggregate and monomer.

10. Computational Screening

First a 2D planar brick lattice is constructed for both the Cy3 and Cy5 dyes, estimating the brick lattice as 2 Å greater than the averaged Cl-Cl distance on the dyes. Then, for a given slip, a 2D planar lattice is generated. For the tube radius as measured by cyro-EM (see Table 2), all possible tube chiral vectors are constructed within a 1 Å tolerance, and then tube Hamiltonian parameters are constructed in the basis of 'stacked rings' of dipoles.[9,10] Examples of acceptable chiral vectors on a Cy5-like dye 2D lattice, and the corresponding tubes generated is shown in Figure 5c.

Parameters for a Cy3- and Cy5-like extended dipole Hamiltonian from a ZINDO calculation of a modified dye, exactly as presented in work from Deshmukh et al.[3,11] Given the predicted inter-ring angle of rotation, γ, a Farey rational approximation for $\gamma/2\pi$ is calculated such that the total number of dyes did not exceed 500,000.[9,12] Using this rational approximation for $\gamma/2\pi$ guarantees good periodic boundaries along the length of the tube, and with a total tube length > 1 μm for all simulations we are fully at the large system limit of the dipole model. Then for each acceptable chiral vector of a given radius, the extended dipole Frenkel Exciton Hamiltonian is constructed, setting the monomer energy equal to zero. At first, we do not treat disorder in the system and in this case, it can be diagonalized by Bloch-waves, which we execute by performing a 2D fast Fourier transform.

A best fit slip and chiral angle was selected for the Cy3-Cl dye and Cy5-Cl dye based off of matching the parallel ($E_0 \rightarrow E(k_z = 0, k_r = 0)$) and perpendicular ($E_{\pm 1} \rightarrow E(k_z = 0, k_r = \pm 1)$) absorption peak shifts from the monomer, as well as, to account for a potential aggregate solid state linear dielectric, the ratio of the peak shifts $E_{\pm 1}/E_0$. Additionally, we can estimate that the tube chiral angle is between 30 and 50° due to the relative oscillator strengths of the parallel and perpendicular peaks in the low temperature experimental spectra, $\frac{f_\perp}{f_\parallel} = \tan^2\theta$ for a disorder free absorption spectrum of a single tube.

Next, the best fit tube Hamiltonian is efficiently screened for disorder using a Chebyshev expansion of the Hamiltonian, until a condition for static disorder leads to a matching peak with of the experimental parallel peak.[13] We select the spectra with the best relative parallel to perpendicular shift, and allow for a linear solid state dielectric scaling to match the total monomer-parallel shift of the tubular aggregate.

11. NMR Spectra

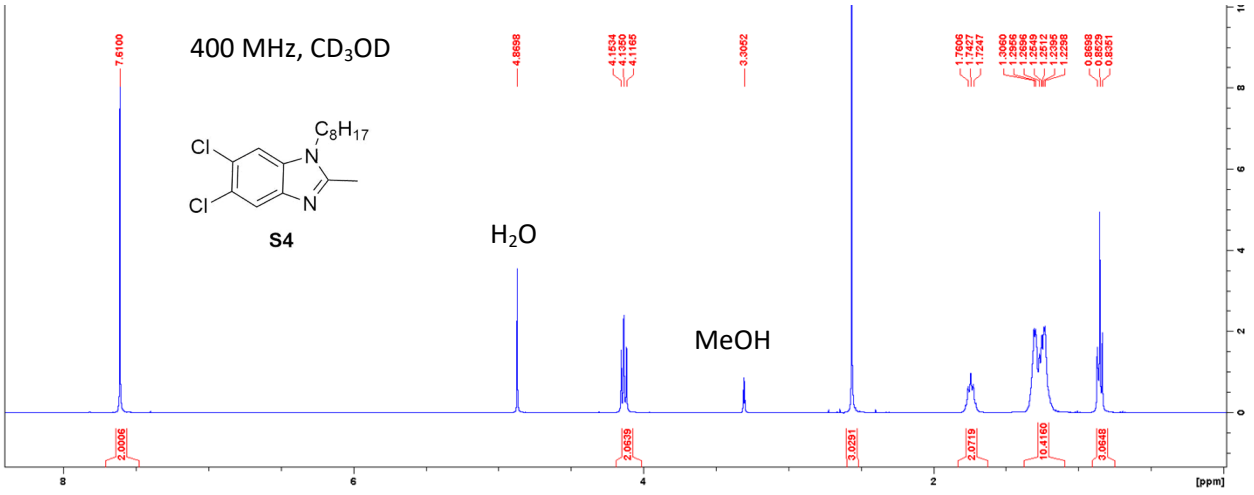

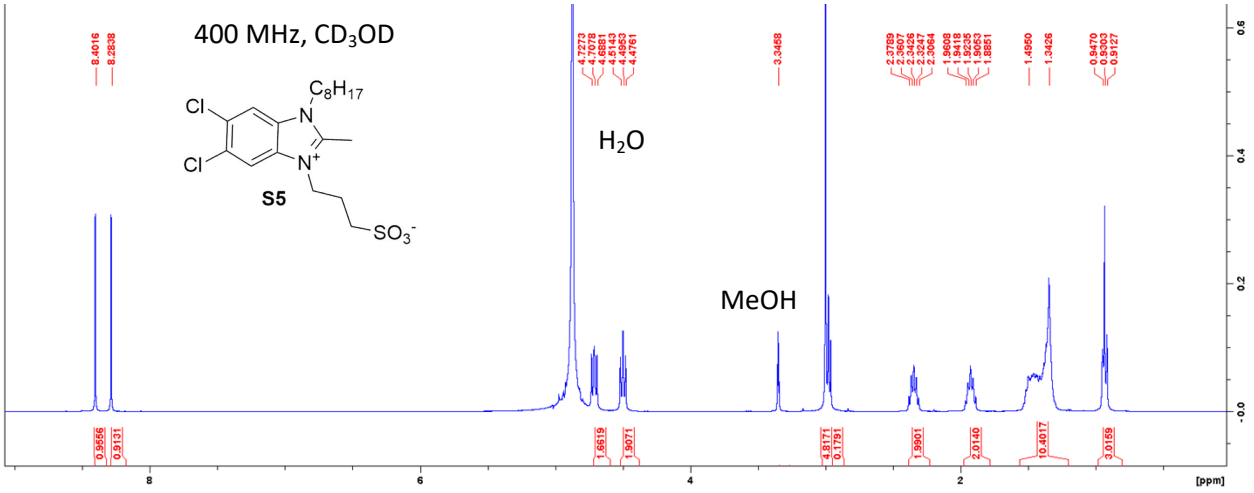

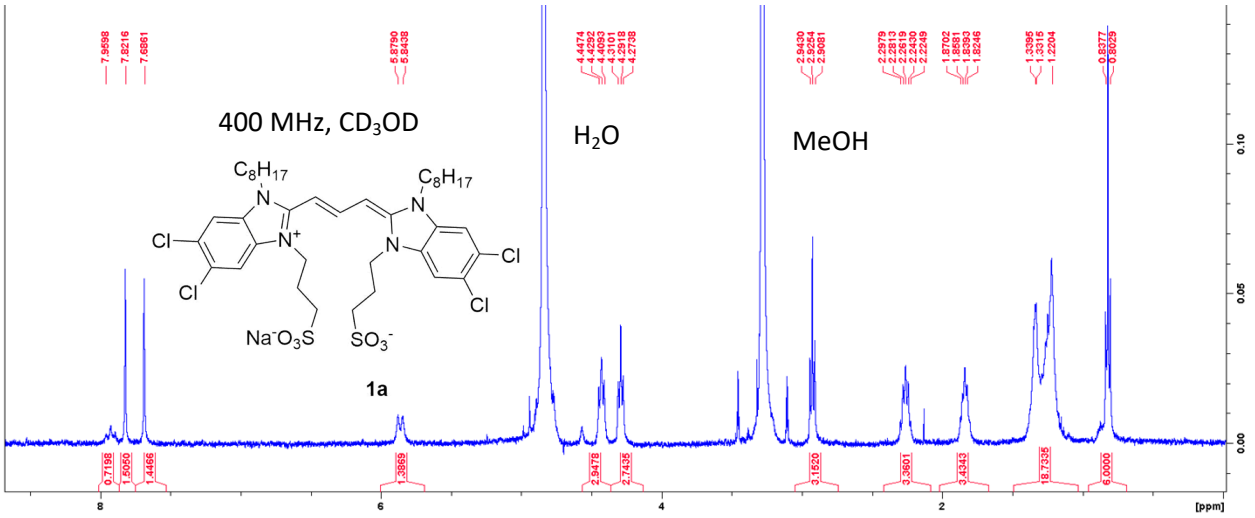
400 MHz, CD3OD
H2O
MeOH
1a
[ppm]

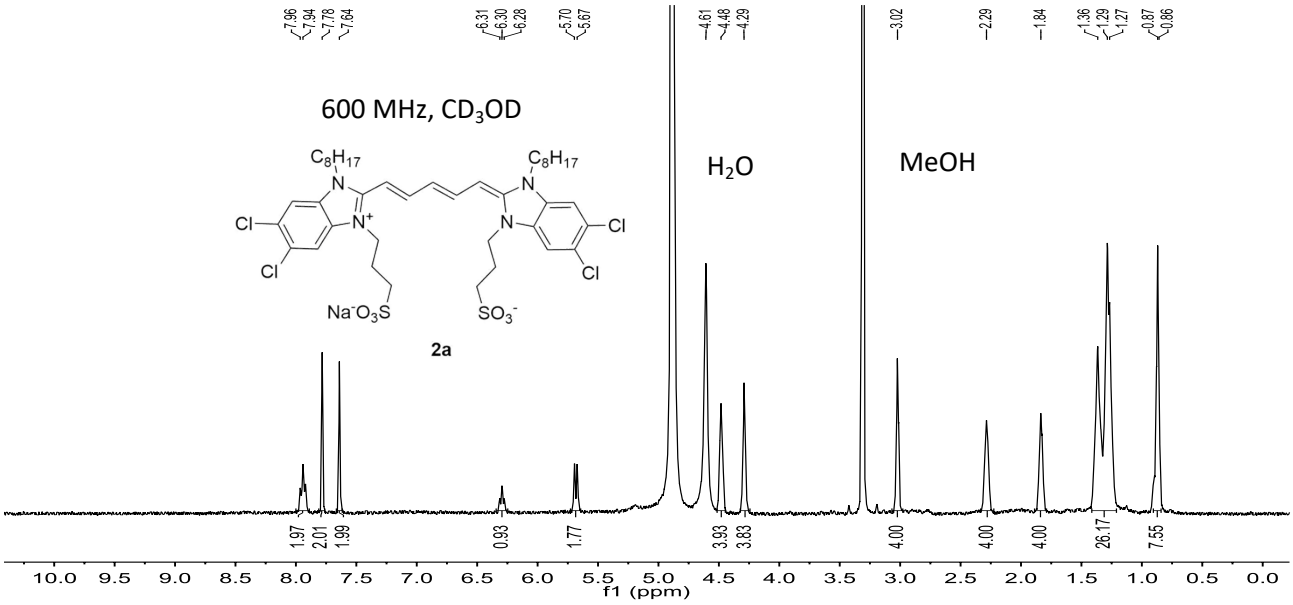
600 MHz, CD3OD
H2O
MeOH
2a
f1 (ppm)

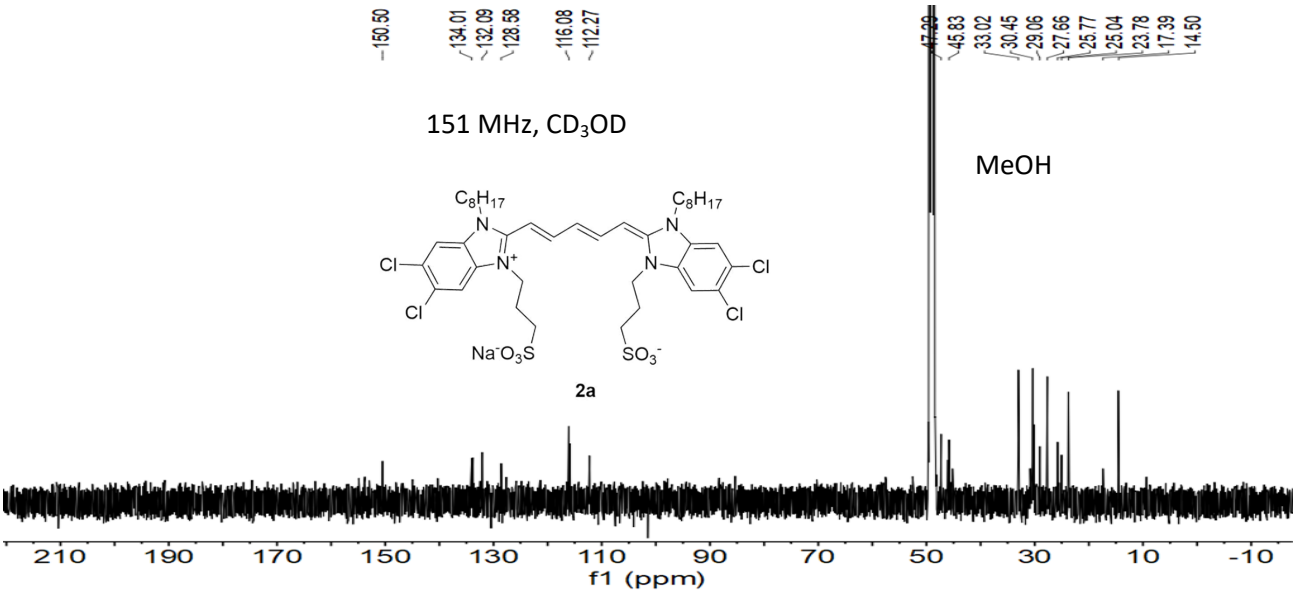
150.50
134.01
132.09
128.58
116.08
112.27
47.39
45.83
33.02
30.45
29.06
27.66
25.77
25.04
23.78
17.39
14.50
151 MHz, CD3OD
MeOH
C8H17
N
N+
Cl
Cl
Na-O3S
SO3-
2a
210
190
170
150
130
110
90
70
50
30
10
-10
f1 (ppm)

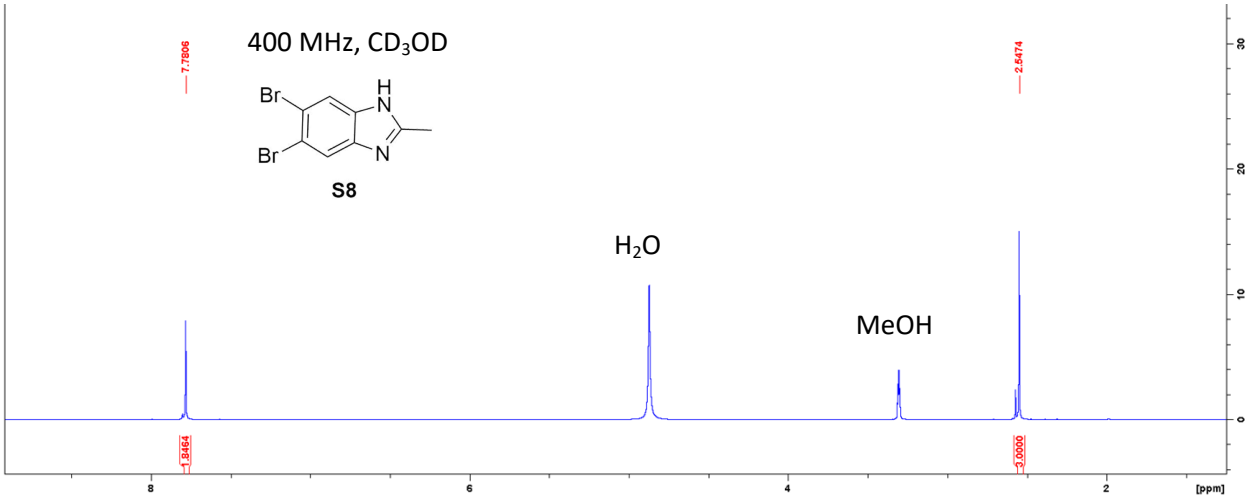
400 MHz, CD3OD
7.7806
2.5474
Br
H
N
S8
H2O
MeOH
1.8464
3.0000
8
6
4
2
[ppm]

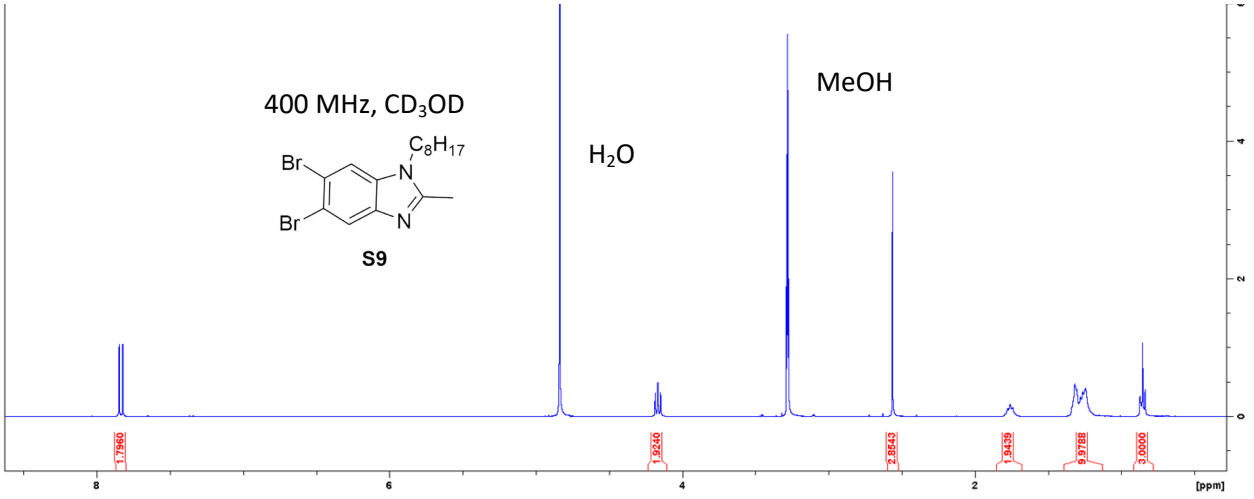
400 MHz, CD3OD
C8H17
Br
N
S9
H2O
MeOH
1.7960
1.9240
2.8543
1.9439
9.9788
3.0000
8
6
4
2
[ppm]

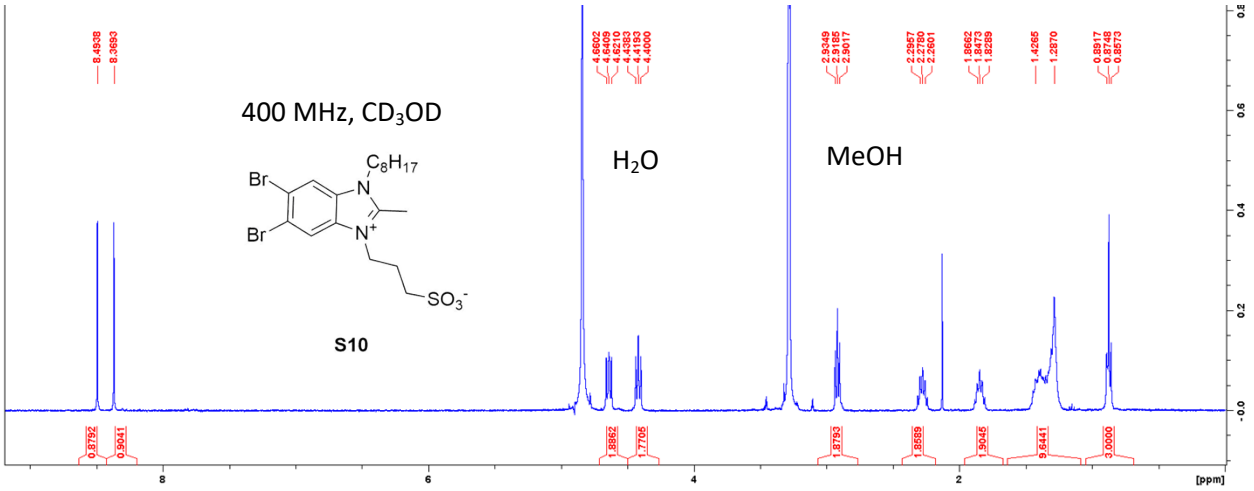
400 MHz, CD_3OD
H_2O
MeOH
S10

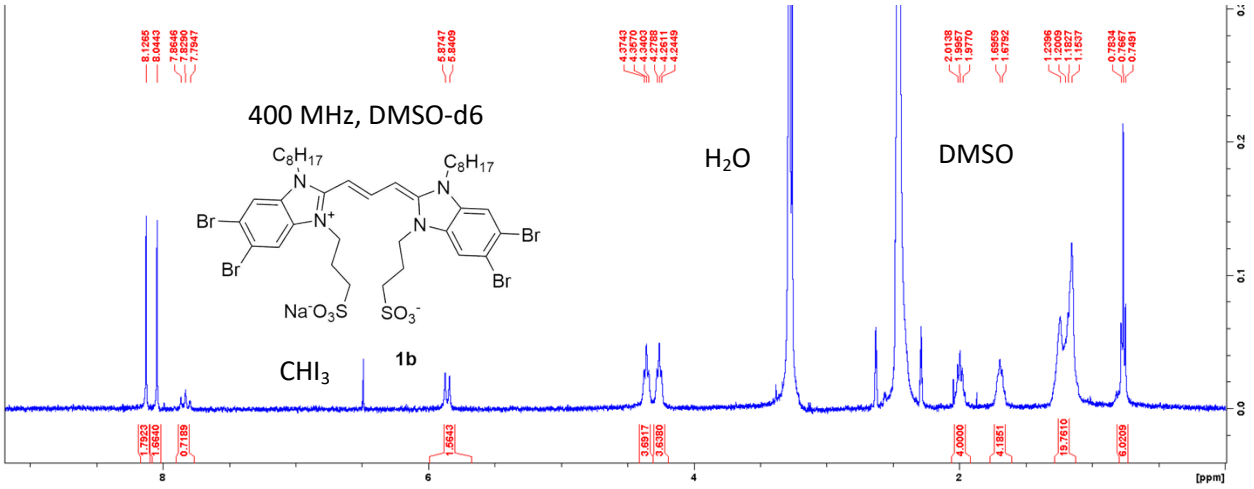
400 MHz, DMSO-d6
H_2O
DMSO
CHI_3
1b

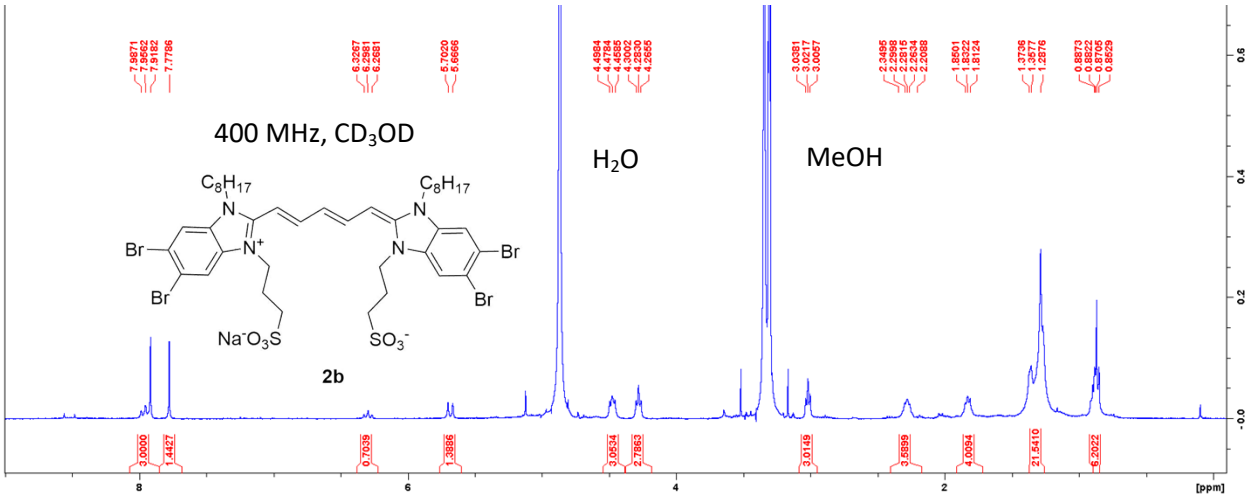
400 MHz, CD_3OD
H_2O
MeOH
2b

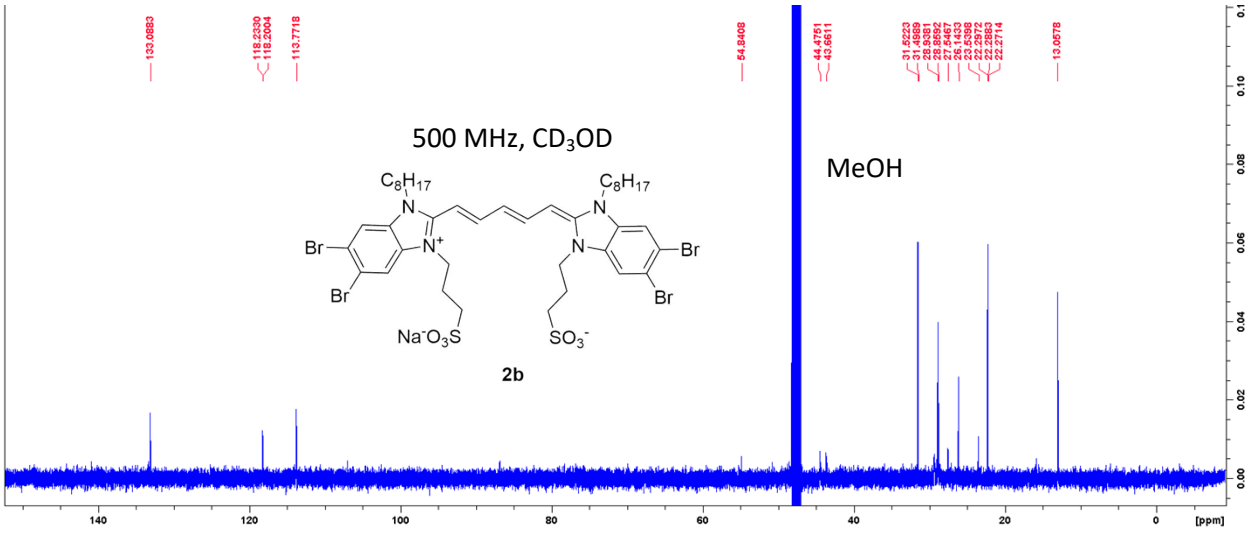

12. References

(1) Pawlik, A.; Ouart, A.; Kirstein, S.; Abraham, H.-W.; Daehne, S. Synthesis and UV/Vis Spectra of J-Aggregating 5,5′,6,6′-Tetrachlorobenzimidacarbocyanine Dyes for Artificial Light-Harvesting Systems and for Asymmetrical Generation of Supramolecular Helices. *Eur. J. Org. Chem.* **2003**, *2003* (16), 3065–3080. https://doi.org/10.1002/ejoc.200300095.

(2) Helmerich, D. A.; Beliu, G.; Matikonda, S. S.; Schnermann, M. J.; Sauer, M. Photoblueing of Organic Dyes Can Cause Artifacts in Super-Resolution Microscopy. *Nat. Methods 2021 183* **2021**, *18* (3), 253–257. https://doi.org/10.1038/s41592-021-01061-2.

(3) Deshmukh, A. P.; Koppel, D.; Chuang, C.; Cadena, D. M.; Cao, J.; Caram, J. R. Design Principles for Two-Dimensional Molecular Aggregates Using Kasha's Model: Tunable Photophysics in Near and Short-Wave Infrared. **2019**. https://doi.org/10.1021/acs.jpcc.9b05060.

(4) Cosco, E. D.; Caram, J. R.; Bruns, O. T.; Franke, D.; Day, R. A.; Farr, E. P.; Bawendi, M. G.; Sletten, E. M. Flavylium Polymethine Fluorophores for Near- and Shortwave Infrared Imaging. *Angew. Chem. Int. Ed.* **2017**, *56* (42), 13126–13129. https://doi.org/10.1002/anie.201706974.

(5) De Mello, J. C.; Wittmann, H. F.; Friend, R. H. An Improved Experimental Determination of External Photoluminescence Quantum Efficiency. *Adv. Mater.* **1997**, *9* (3), 230–232. https://doi.org/10.1002/adma.19970090308.

(6) Atallah, T. L.; Sica, A. V.; Shin, A. J.; Friedman, H. C.; Kahrobai, Y. K.; Caram, J. R. Decay-Associated Fourier Spectroscopy: Visible to Shortwave Infrared Time-Resolved Photoluminescence Spectra. *J. Phys. Chem. A* **2019**, *123* (31), 6792–6798. https://doi.org/10.1021/acs.jpca.9b04924.

(7) Sillen, A.; Engelborghs, Y. The Correct Use of "Average" Fluorescence Parameters. *Photochem. Photobiol.* **1998**, *67* (5), 475–486. https://doi.org/10.1111/j.1751-1097.1998.tb09082.x.

(8) Friedman, H.; Cosco, E.; Atallah, T.; Jia, S.; Sletten, E.; Caram, J. Establishing Design Principles for Emissive Organic SWIR Chromophores from Energy Gap Laws. **2021**. https://doi.org/10.26434/CHEMRXIV.14374493.V1.

(9) Didraga, C.; Klugkist, J. A.; Knoester, J. Optical Properties of Helical Cylindrical Molecular Aggregates: The Homogeneous Limit. *J. Phys. Chem. B* **2002**, *106* (44), 11474–11486. https://doi.org/10.1021/JP026217S/ASSET/IMAGES/LARGE/JP026217SF00007.JPEG.

(10) Didraga, C.; Pugžlys, A.; Hania, P. R.; Von Berlepsch, H.; Duppen, K.; Knoester, J. Structure, Spectroscopy, and Microscopic Model of Tubular Carbocyanine Dye Aggregates. *J. Phys. Chem. B* **2004**, *108* (39), 14976–14985. https://doi.org/10.1021/JP048288S/ASSET/IMAGES/MEDIUM/JP048288SE00023.GIF.

(11) Deshmukh, A. P.; Geue, N.; Bradbury, N. C.; Atallah, T. L.; Chuang, C.; Pengshung, M.; Cao, J.; Sletten, E. M.; Neuhauser, D.; Caram, J. R. Bridging the Gap between H- and J-Aggregates: Classification and

Supramolecular Tunability for Excitonic Band Structures in Two-Dimensional Molecular Aggregates. *Chem. Phys. Rev.* **2022**, *3* (2), 021401. https://doi.org/10.1063/5.0094451.
(12) Guthery, Scott. *A Motif of Mathematics: History and Application of the Mediant and the Farey Sequence*; Docent Press: North Charleston, SC, 2011.
(13) *Stochastically Realized Observables for Excitonic Molecular Aggregates | The Journal of Physical Chemistry A*. https://pubs.acs.org/doi/10.1021/acs.jpca.0c07953 (accessed 2022-09-05).